# Decay of nuclear magnetization by bounded diffusion in a constant field gradient

Thomas M. de Swiet
*Department of Physics, Harvard University, Cambridge, Massachusetts 02138 and Schlumberger–Doll Research, Old Quarry Road, Ridgefield, Connecticut 06877-4108*

Pabitra N. Sen
*Schlumberger–Doll Research, Old Quarry Road, Ridgefield, Connecticut 06877-4108*

(Received 19 November 1993; accepted 6 January 1994)

Transverse magnetization of spins diffusing in a bounded region in the presence of a constant field gradient is studied. We investigate the breakdown at short times of the much used formula for the Hahn echo amplitude in a constant gradient in unbounded space: $\mathcal{M}(2\tau)/\mathcal{M}(0)=\exp(-2D_0g^2\tau^3/3)$. Here $D_0$ is the diffusion constant in unbounded space and $g$ is the field gradient multiplied by the gyromagnetic ratio. We find that this formula is replaced by $\mathcal{M}(2\tau)/\mathcal{M}(0)=\exp[-2D_{\text{eff}}g^2\tau^3/3+\mathcal{O}(D_0^{5/2}g^4\tau^{13/2}S/V)]$ with an effective diffusion coefficient $D_{\text{eff}}(2\tau) = D_0[1 - \alpha\sqrt{D_0\tau}(S/V) + \cdots]$, where $\alpha$ is a constant and $S/V$ is the surface to volume ratio of the bounded region. Breakdown is complex but we find that the interplay between a natural length scale $l_c=(g/D_0)^{-1/3}$ and the geometry of the region governs the problem. The long-time behavior of the free induction decay and echo amplitude are then considered where pure $\exp[-\text{const}\,t]$ decay is expected. We consider some simple geometries and find in addition to the well-known result, $\ln|M(z,t)|\sim -D_0g^2R_p^4t$, valid for $R_p \ll l_c$ (where $R_p$ is the size of the confining space) that in the regime $R_p \gg l_c$ the decay becomes $\ln|M(z,t)|\sim -g^{2/3}D_0^{1/3}t$. We then argue that this latter result should apply to more general geometries. We discuss implications for realistic experimental echo measurements and conclude that the $g^{2/3}D_0^{1/3}$ decay regime is hard to measure. Implications for the effect of edge enhancement in NMR microscopy are also discussed.

## I. INTRODUCTION

The purpose of this paper is to study some of the complex range of phenomena resulting from the combined effects of diffusion, field gradients, and restricted geometries on NMR measurements.

Microscopic field gradients arise in practically all experimental situations due to variation in susceptibility within the sample.[1] This can arise through the contrast between pore space and grain in rocks or typically in biological systems the contrast between tissue and fluid. In many rocks dephasing of spins due to their diffusive motion in these gradients is the dominant process resulting in attenuation of the Hahn echo amplitude. Understanding such effects of microscopic field inhomogeneity is important because they cannot always be removed by appropriate pulse sequences and in any case contain potentially useful information about the sample.

Macroscopic gradients also occur in a variety of experiments. In nuclear magnetic resonance imaging NMRI spatial encoding is performed through application of magnetic field gradients. The effects of restricted diffusion in these gradients have recently received more attention both in so-called diffusion weighted imaging and in NMR microscopy as resolution is pushed down to the micron region and thus diffusive length scales. One particularly interesting phenomenon is the diffusive enhancement of images near the boundaries of the system which are perpendicular to the gradient direction. This edge enhancement opens the way to resolution of restrictions to diffusion of arbitrary thickness as has been demonstrated in the experiments of Callaghan *et al.*[2]

Pulsed field gradient spin echo (PFGSE), experiments also involve application of macroscopic field gradient pulses. Diffusion during these gradient pulses needs to be accounted for in explaining results even at relatively small $k$ values.[3] At large $k$ values diffusion generally dominates since to obtain large $k$ values long pulses are required. Even inhomogeneity in the dc background field of the magnet is an important issue which is not easily circumvented by pulse sequences.

Previous work on restricted diffusion in inhomogeneous fields has mostly relied on the Gaussian phase approximation.[4–6] This is shown below only to be valid in either in the limit of short times or in the limit of fast diffusion at long times. Le Doussal and Sen[7] have studied the exact solution of diffusion of spins in field gradients which feel a harmonic restoring force, however, this can only be a crude model of the abrupt barriers present in experimental situations. Stoller *et al.*[8] have discussed in detail the case of spins confined in the one-dimensional slab geometry with a uniform field gradient. This work forms the basis for understanding the non-Gaussian regime in more complicated geometries.

In this paper we concentrate on the Hahn echo experiment for spins diffusing in systems of the following type. The applied field has a constant gradient, the spins are free to diffuse in some bounded region (not necessarily connected) to be known as the pore space from the walls of which they are reflected, and the initial concentration of spins is taken to be uniform.

In Sec. II we discuss the well-known formula[9] valid for unbounded space:

$$\mathcal{M}(2\tau)/\mathcal{M}(0)=\exp(-2D_0g^2\tau^3/3). \tag{1}$$

This formula is often used when considering bounded regions in the hope that at short enough times the spins do not see the boundaries. (See, e.g., Ref. 10). An important issue is the range of validity of this result. By expanding around the Gaussian phase approximation we find under general conditions that at short echo times the Hahn echo amplitude

$$\ln[\mathscr{M}(2\tau)/\mathscr{M}_0]=-\tfrac{2}{3}g^2\tau^3D_0[1-\alpha(S/V)\sqrt{D_0\tau}+\mathscr{O}(D_0\tau)] +\mathscr{O}(D_0^{5/2}g^4\tau^{13/2}S/V)$$

where

$$\alpha=32(2\sqrt{2}-1)/105\sqrt{\pi},g=\gamma\nabla B_z,$$

$D_0$ is the bulk diffusion coefficient, $2\tau$ is the echo time, and $S/V$ is the pore space surface to volume ratio. We argue that the unbounded space result is valid until spins diffuse across the pore or over the intrinsic length scale of the field gradient $l_c=(g/D_0)^{-1/3}$, whichever occurs sooner. $l_c$ may be thought of as the typical length scale over which a spin must travel to dephase by $2\pi$ radians.

After the unbounded space result breaks down the echo amplitude should eventually cross over to a pure exponential decay. For simplicity we first consider the related long-time behavior of the free induction decay. In simple geometries with a well defined size "$R_p$" there are two clear regimes in which the long-time decay rate takes a simple form. In Sec. III A we briefly consider the previously studied[4,11,12] fast diffusion regime where $l_c\gg R_p$ and describe how it can also be understood through the Gaussian phase approximation. Although the fast diffusion regime has received more attention[13] in the analysis of experiment, the asymptotic limit $l_c\ll R_p$ is also relevant—it is certainly the domain of edge enhancement in images. In a typical rock this regime will be realized for some of the pores since $l_c$ due to the microscopic gradients alone is of the order microns.

In Sec. III B we discuss the case $l_c\ll R_p$ in the one-dimensional slab geometry which is treated exactly in Ref. 8. In Sec. III C we build on this first to consider the regime $l_c\ll R_p$ in cylindrical and spherical geometries and then to argue that the results should be generalizable to more complex pore spaces. In particular, in the small $l_c$ limit we expect a universal decay rate $\ln|M(z,t)|\sim -E_1g^{2/3}D_0^{1/3}t$ where $E_1$ is a constant $\sim 0.5094$.

In Sec. IV we consider how the results of Sec. III determine the behavior of the Hahn echo experiment at long times. We find that in the small $l_c$ limit the pure exponential decay region occurs at increasingly weak signal so that the universal result may never be measured outside rather artificial geometries. We make qualitative arguments to suggest that $l_c$ sets a limit on the effective pore size in the gradient direction.

In Sec. V we discuss the phenomenon of edge enhancement that occurs in imaging experiments where the resolution is of the order $l_c$ and $l_c\ll R_p$. This is a subject which has been understood until now only in a heuristic fashion.[2,14,15] We are able to clarify the physics and make some quantitative statements about previous numerical and experimental results.

## II. SHORT-TIME BEHAVIOR OF THE HAHN ECHO AND THE GAUSSIAN PHASE APPROXIMATION

In this section we show how the Gaussian phase approximation can be used to find the behavior of the Hahn echo amplitude at short times in a general confined space. We then discuss the range of validity of Eq. (1). This result is only strictly correct in unbounded space and is perhaps the most used result for the behavior of the Hahn echo envelope in the presence of a field gradient. Note that this method cannot be used to find the form of the free induction decay which is sensitive to details of the geometry even at the shortest times.

The free induction decay or measured transverse magnetization in an NMR experiment after a $\pi/2$ pulse may be written, in the presence of a field gradient, as

$$M(t)=M(0)\int P(\phi)e^{i\phi}\,d\phi, \tag{2}$$

where $M=M_x+iM_y$ and $M(0)$ is the signal directly after the $\pi/2$ pulse. The effect of the bulk $T_2$ has not been explicitly displayed since it simply has the effect of multiplying $M(t)$ by $\exp(-t/T_2)$. $P(\phi)$ is the probability density of a spin having acquired a relative phase $\phi$ due to its Brownian path in the inhomogeneous field. The relative phase of a spin in a uniform field gradient is given by $\phi(t)=-g\int_0^t x_i(t)dt$, where $x_i(t)$ is the Cartesian coordinate of the spin in the direction of the field gradient and $g=\gamma|\nabla B_z|$. Note that only the gradient of the large component of magnetic field contributes. Gradients, if any, of the small transverse components are rapidly fluctuating in the rotating frame of the spin. It can be seen immediately that if we are to know $P(\phi)$ we must know the distribution of $x$ coordinates $P(x_i)$ which is clearly dependent on the geometrical details of the bounded space at all times.

Now in the Hahn echo experiment we apply a $\pi$ pulse at $t=\tau$ which has the effect of negating the phase accumulated up until that time so that at time $t=2\tau$ the accumulated phase is $\phi(2\tau)=g\int_0^\tau x_i(t)dt-g\int_\tau^{2\tau}x_i(t)dt$ or equivalently $\phi(2\tau)=g\int_0^\tau[x_i(t)-x(0)]dt-g\int_\tau^{2\tau}[x_i(t)-x(0)]dt$. We are now concerned with $x_i(t)-x_i(0)$ which is well known to have a Gaussian distribution in unbounded space. At short times only a small fraction of spins have encountered the walls so, although we can say very little about the distribution of $x(t)$ in an arbitrary confined geometry, the distribution of $x_i(t)-x_i(0)$ or of displacements must be Gaussian at short enough times. By a general theorem if $x_i(t)-x_i(0)$ is a Gaussian stochastic process any linear transformation also yields a Gaussian process. We therefore expect that precisely at the echo time $2\tau$ that the distribution of phases $P(\phi)$ will be Gaussian for small $\tau$.

In this situation it is natural to perform a cumulant expansion of the distribution of phases. Taking the logarithm of Eq. (2) we obtain

$$\ln[M(t)/M(0)]=-\langle\phi^2\rangle/2+\langle\phi^4\rangle/4!-\langle\phi^2\rangle^2/8+\cdots. \tag{3}$$

Here we have assumed that the confining geometry has inversion symmetry so that averages of odd powers of $\phi$ van-

ish. We must now find the behavior of successive cumulants at short times. We may calculate the second cumulant as follows:

$$\langle\phi^2(2\tau)\rangle = g^2\left[\int_0^\tau\int_0^\tau + \int_\tau^{2\tau}\int_\tau^{2\tau} - 2\int_0^\tau\int_\tau^{2\tau}\right] \times\langle x(t)x(t')\rangle dt\, dt'. \tag{4}$$

Now

$$\langle x(t)x(t')\rangle = -1/2\langle[x(t)-x(t')]^2\rangle + 1/2[\langle x^2(t)\rangle + \langle x^2(t')\rangle]. \tag{5}$$

Since we assume a uniform initial concentration of spins and we have reflecting boundary conditions $\langle x^2(t)\rangle$ is independent of time and $\langle[x(t)-x(t')]^2\rangle$ is only a function of $t-t'$. Mitra *et al.*[16] have shown $\langle[x(t)-x(0)]^2\rangle$ has the expansion

$$\frac{\langle[\mathbf{r}(t)-\mathbf{r}(0)]^2\rangle}{6t} = D_0\left[1-\frac{4S\sqrt{D_0t}}{9V\sqrt{\pi}} + \mathcal{O}(D_0t)\right], \tag{6}$$

where $S/V$ is the surface to volume ratio of the pore space. Note that other length scales come in at higher orders of $\sqrt{D_0t}$ such as the mean curvature of the pore walls. If we assume a pore space which is isotropic, at least on the average, $\langle[x(t)-x(0)]^2\rangle$ is simply one-third of this. Putting this into Eqs. (5) and (4) we find

$$\frac{\langle\phi^2(2\tau)\rangle}{2} = \frac{2\gamma^2g^2\tau^3D_0}{3}\left[1-\frac{\alpha S\sqrt{D_0\tau}}{V} + \mathcal{O}(D_0\tau)\right], \tag{7}$$

where $\alpha = 32(2\sqrt{2}-1)/105\sqrt{\pi}$.

Next we must consider the behavior of the fourth cumulant $\langle\phi^4(2\tau)\rangle/24 - \langle\phi^2(2\tau)\rangle^2/8$. Since this is zero in unbounded space it is clear that to lowest order in $\tau$, $\langle\phi^4(2\tau)\rangle \sim D_0^2g^4\tau^6$. In fact the methods of Mitra *et al.* can be generalized by a rather tedious calculation[17] to expand

$$\langle[x(t_1)-x(0)][x(t_2)-x(0)][x(t_3)-x(0)][x(t_4)-x(0)]\rangle$$

at short times, yielding

$$\langle\phi^4(2\tau)\rangle/24 - \langle\phi^2(2\tau)\rangle^2/8 \sim D_0^{5/2}g^4\tau^{13/2}S/V. \tag{8}$$

Putting Eqs. (7) and (8) into Eq. (3), the final result is

$$\ln[M(2\tau)/M_0] = -\frac{2g^2\tau^3D_0}{3}\left[1-\frac{\alpha S\sqrt{D_0\tau}}{V} + \mathcal{O}(D_0\tau)\right] + \mathcal{O}(D_0^{5/2}g^4\tau^{13/2}S/V). \tag{9}$$

Thus the cumulant expansion becomes an expansion in $g$ and $\tau$. The free space result is rigorously shown to be asymptotically correct at short times. The breakdown of this formula is rather complicated especially when we consider that other length scales such as the mean curvature of the walls come into play at the next order from the surface to volume ratio. However, there are two clear modes of breakdown. The first is where the Gaussian phase approximation remains valid but terms like $\sqrt{D_0\tau}/R_p$ become of order unity, where by $R_p$ we mean some averaged geometrical length like those given by surface to volume ratio or mean curvature. The second is when the higher cumulants become important. Analysis of higher order terms[17] suggests that, neglecting slowly varying terms $q$ the form $\ln(R_p/l_c)$, this occurs when $g^2\tau^3D_0$ becomes of order unity. Stated in terms of diffusion length the first is when the diffusion length is of order $R_p$, the second when it is of order $l_c=(g/D_0)^{-1/3}$. The first dominates the second when $R_p \ll l_c$ and vice versa.

## III. THE TORREY EQUATION AND THE LONG-TIME BEHAVIOR OF THE MAGNETIZATION

In this section we discuss the long-time behavior of the free induction decay.

At long times it is natural to focus on the magnetization as evolving under a governing differential equation, rather than as a sum over paths, due to the need to apply hard boundary conditions at the walls of the pore space. The transverse magnetization density $M=M_x+iM_y$, following a $\pi/2$ pulse, obeys Bloch's equation as modified by Torrey,[18] to include diffusion:

$$\frac{\partial M(\mathbf{r},t)}{\partial t} = D_0\nabla^2M(\mathbf{r},t) - i\mathbf{g}\cdot\mathbf{r}M(\mathbf{r},t) \tag{10}$$

with the initial condition that $M(\mathbf{r},0)=$const. A factor of $\exp(-i\omega_0-1/T_2)t$ has been divided out of $M(\mathbf{r},t)$ where $\omega_0=\gamma B_0$, the average Larmor frequency. Here $D_0$ is the diffusion constant, $\mathbf{g}$ is the gyromagnetic ratio multiplied by the local gradient of the background field, $\mathbf{g}=\gamma\nabla B_z$, and $T_2$ is the bulk decay rate.

The above equation has an intrinsic length scale:

$$l_c=(g/D_0)^{-1/3}. \tag{11}$$

As a result in simple geometries, where there is a single geometrical length $R_p$, one dimensionless parameter $l_c/R_p$ characterizes the solutions. Separating out the time dependence we obtain the eigenvalue equation

$$-D_0\nabla^2m_i(\mathbf{r}) + i\gamma\mathbf{g}\cdot\mathbf{r}m_i(\mathbf{r}) = E_im_i \tag{12}$$

with the general solution for the magnetization

$$M(\mathbf{r},t) = \sum c_im_i(\mathbf{r})e^{-E_it}. \tag{13}$$

Note that this solution will strictly break down for certain special values of $l_c/R_p$ due to the non-Hermiticity of the eigenvalue operator as shown by Stoller *et al.* for the one-dimensional case.[8] We are interested in solution of Eq. (12) in a confined space under reflecting boundary conditions. At long times the magnetization is well described by the eigenstate with the smallest real part to its eigenvalue and decays with a pure exponential. In all but one dimension, Eq. (12) cannot be solved exactly. In Sec. III A we discuss the decay rate for $l_c \gg R_p$ in simple geometries. In Sec. III B we discuss $l_c \ll R_p$, focusing on one dimension which is then extended to higher dimension and more complex spaces in Sec. III C.

### A. The fast diffusion limit

Much attention has been paid to the case where $l_c/R_p$ is large.[4,11,12] In this regime one can expand around the eigenfunctions and eigenvalues of the diffusion equation with a

perturbation series in $(R_p/l_c)^6$. [Although $(R_p/l_c)^3$ is what enters the nondimensionalized time-independent Torrey equation odd powers do not enter the perturbation series if we assume inversion symmetry.] Since the lowest eigenstate of the unperturbed time-independent diffusion equation is always just a constant with zero decay rate $E_i$, we recover that the dimensionless long-time decay rate goes like $(R_p/l_c)^6$ or when we redimensionalize, $g^2R_p^4/D_0$.

Now consider when this long-time decay rate sets in. We have only described a small perturbation around the diffusive decay rates so that the gross separation of successive decay rates is still given by the diffusive scale $E_i-E_j\sim D_0/R_p^2$. This separation determines the time at which the lowest eigenstate dominates and there is crossover to the pure exponential regime; i.e., when $\exp[-(E_i-E_j)t]\ll 1$. Recall that $t\sim R_p^2/D_0$ is also the time scale at which the unbounded space result for the spin echo breaks down if $l_c\gg R_p$.

Since the eigenvalues are still real to all orders in perturbation theory, another way to think of this regime is as the motional narrowing limit because the frequency spectrum is a series of Lorentzians centered at the average frequency of the container. Thus there is no frequency resolution of the container.

The same form for the magnetization at long times is also obtained by applying the Gaussian phase approximation as in Sec. II in the limit of long times. This can be seen as follows. Once a spin has traversed the container several times it has clearly lost its memory of where it started. Thus at long times we can regard the accumulated phase of an individual spin as a sum of many small independent errors which represent the phase accumulated over a few traversals of the container. Under these conditions by the central limit theorem we expect the distribution of phases to tend to a Gaussian at long times. However, there is a set time scale over which spin dephasing occurs which is the time required to diffuse $l_c$. This is equivalent to saying that we only care about the phase modulo $2\pi$. Thus we need the additional requirement for the Gaussian phase approximation to hold—that the time to diffuse $l_c$ is much greater than the traversal time or $l_c\gg R_p$. Thus the calculations of Neumann[4] using the Gaussian phase approximation reproduce the theoretical results for the long-time decay rate of Robertson[12] and others valid in this regime and are in agreement with experiment.[11]

### B. The slow diffusion limit in one dimension

We focus on the case where $l_c/R_p$ is small. In this situation spins do not typically diffuse across the whole container before they are dephased. The dominant eigenstates at long times are localized near to that portion of the wall which is perpendicular to the gradient. It is here that there is most restriction to diffusion along the gradient direction and thus dephasing is minimized.

We now discuss the one-dimensional slab geometry. Although the Torrey equation in one dimension has been solved exactly by Stoller *et al.*,[8] we repeat here some of the relevant details emphasizing the asymptotic behavior of the solutions for small $l_c/R_p$.

In this geometry $R_p$ is taken as the width of the slab. Define new variables:

$$\hat{x}=\left(\frac{g}{D_0}\right)^{1/3}x,\quad \hat{E}=\frac{E_i}{D_0^{1/3}g^{2/3}},\quad z\equiv\hat{E}-i\hat{x}. \tag{14}$$

Then in one dimension with no surface relaxation, Eq. (12) becomes Airy's equation

$$\frac{d^2m_i}{dz^2}=m_iz;\quad \frac{dm_i}{dz}=0\quad \text{if } z=\hat{E}\pm i\,\frac{R_p}{2l_c}. \tag{15}$$

A choice for the two linearly independent solutions is $\mathrm{Ai}(e^{2\pi i/3}z)$ and $\mathrm{Ai}(e^{-2\pi i/3}z)$.[19] These have the property of decaying exponentially for the imaginary part of $z$ large and negative or large and positive, respectively, and are, individually, the correct solutions for left and right bounded half-spaces. Although the solution of Eq. (15) is strictly a linear combination of both of these terms, to a first approximation each solves Eq. (15) separately when $R_p$ is large. This is simply because states localized at one wall do not "see" the other wall where they are exponentially small. The decay rates $\hat{E}$ are then determined by the equation $\mathrm{Ai}'[e^{\pm 2\pi i/3}(\pm iR_p/2l_c+\hat{E})]=0$. The zeros $\{a_i\}$ of Ai′ are real and negative ($a_1=-1.0188$, $a_2=-3.2482$, $a_3=-4.8201$, etc.). So to this approximation the eigenfunctions are a set of functions localized at the left wall, $\mathrm{Ai}(e^{+2\pi i/3}z)$, with $\hat{E}=e^{-2\pi i/3}a_i-iR_p/2l_c$ and a set at the right wall. From now on we will only calculate the left wall states. The right wall states are simply obtained from the symmetry of Eq. (15): For every left wall state $m_i(\hat{x})$, decay rate $\hat{E}$ there is a right wall state $m_i^*(-\hat{x})$, decay rate $\hat{E}^*$. This is intuitively obvious—the left and right wall states decay at the same rate but are frequency shifted by opposite amounts from the average.

These states can be used as the basis of a perturbation expansion with the small parameter being $\epsilon\equiv l_c/R_p$. The exact decay rates are determined by

$$\begin{aligned}&\mathrm{Ai}'[e^{2\pi i/3}(iR_p/2l_c+\hat{E})]\mathrm{Ai}'[e^{-2\pi i/3}(-iR_p/2l_c+\hat{E})]\\&\quad=\mathrm{Ai}'[e^{2\pi i/3}(-iR_p/2l_c+\hat{E})]\\&\qquad\times\mathrm{Ai}'[e^{-2\pi i/3}(iR_p/2l_c+\hat{E})].\end{aligned} \tag{16}$$

This can be solved perturbatively in the usual manner to yield the following complex expression for left wall states:

$$E_i=D^{1/3}g^{2/3}\left[\frac{-i}{2\epsilon}+e^{-2\pi i/3}a_i+i\,\frac{\mathrm{Ai}'(e^{-4\pi i/3}a_i)}{\mathrm{Ai}''(a_i)}\times\exp\left[-\frac{\epsilon^{-3/2}(1+i)}{\sqrt{2}}\right]\right]. \tag{17}$$

Note that the correction to the one wall decay rate is "transcendentally small" so that the one wall expression should be accurate for quite modest values of $R_p/l_c$. Unfortunately, this rapid convergence is a one-dimensional artifact as will be shown below. Note that the leading term is purely imaginary and thus represents oscillation as opposed to decay. This simply represents the gross frequency shift of a state localized near the wall from the average which is the Larmor frequency at the center of the slab. The corrections to the eigenstates are transcendentally small amounts of right wall state mixed into the left ones and vice versa.

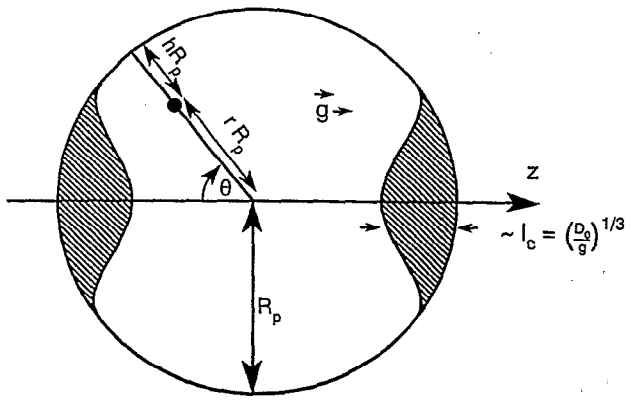


FIG. 1. Coordinate system used for the Torrey equation in the cylindrical geometry. The longest lived eigenstates are shown schematically.

An important point is that this approximation scheme assumes $a_i$ is of order 1. It is always possible to find delocalized eigenstates with $a_i$ of order $1/\epsilon$ for which the perturbation theory breaks down. However, these of course decay quickly and are not relevant to the long-time behavior. Another way to understand this is that the formula above for the left wall states gives a sequence of states gradually frequency shifted further and further to the right of the left wall. Clearly this cannot go on indefinitely. In fact what is shown in the exact calculation of Stoller *et al.* is that at any finite value of $\epsilon$ there is only a finite number of states which are frequency shifted at all. The rest have purely real eigenvalues and are thus centered at the average frequency of the box (but are delocalized in space).

### C. The slow diffusion limit in higher dimension

In two dimensions the prototypical geometry is cylindrical. $R_p$ is now taken to be the radius of the cylinder. We again look for solutions of the time-independent Torrey equation with reflecting boundary conditions for small $l_c/R_p$. We nondimensionalize Eq. (12) by scaling all lengths by $R_p$ and the decay rate $E'=E_i/R_pg$. Working in polar coordinates define the variable $h$ to be $1-r$ where $r$ is the scaled radial coordinate. (See Fig. 1.) We then obtain

$$-\epsilon^3\left(\frac{\partial^2 m_i}{\partial h^2}-\frac{1}{1-h}\frac{\partial m_i}{\partial h}+\frac{\partial^2 m_i}{\partial \theta^2}\right)+im_i[1-(1-h)\cos\theta]$$
$$=(E'+i)m_i. \tag{18}$$

We were not able to solve this equation for finite $\epsilon$. However, for small $\epsilon$ we expect that the long-lived eigenstates are squashed up against the edge of the circle and confined to values of $\theta$ near 0 and $\pi$. We will concentrate on states with values of $\theta$ near 0—those near $\pi$ just being complex conjugates. It is natural in this situation to use the ideas of boundary layer theory. The outer solution is clearly $m_i=0$ which means simply that the inner solution must go to zero for large $h$, $|\theta|$. From experience with the one-dimensional problem we would only expect to incur exponentially small error from this assumption. The only possible scaling of coordinates within the boundary layer that leads to nontrivial solutions is $h'=h/\epsilon$ and $\theta'=\theta/\epsilon^{3/4}$. We then take

$$E+i=E_0\epsilon+E_1\epsilon^{3/2}+E_2\epsilon^2+\cdots, \tag{19}$$

$$m_i=m_0+m_1\epsilon+m_2\epsilon^2+\cdots. \tag{20}$$

The given expansions and scalings may need to be adjusted at higher order but are correct to obtain the lowest-order approximation for the eigenfunction and lowest two orders of approximation for the eigenvalue. We then obtain to order $\epsilon$:

$$-\frac{\partial^2 m_0}{\partial h'^2}+im_0h=E_0m_0. \tag{21}$$

So we find $m_0=\mathrm{Ai}[e^{2\pi i/3}(E_0-ih')]f(\theta')$ and $E_0=e^{-2\pi i/3}a_i$. To order $\epsilon^{3/2}$ we obtain

$$-\frac{\partial^2 m_0}{\partial \theta'^2}+im_0\theta'^2=+E_1m_0. \tag{22}$$

We see $E_1=(n+1/2)(1+i)$ where $n$ is an integer $\geq 0$ and $f(\theta')=\exp[-(1+i)\theta'^2/2]H_n(\sqrt{1+i}\,\theta')$, where $H_m$ are Hermite polynomials of order $m$. On redimensionalizing we obtain for the left wall states

$$E_{i,n}=-iR_pg+g^{2/3}D_0^{1/3}e^{-2\pi i/3}a_i+\sqrt{gD_0/R_p}(n+1/2)$$
$$\times(1+i)+\mathcal{O}(g^{1/3}D_0^{2/3}/R_p). \tag{23}$$

The noteworthy features of Eq. (23) are that it is only valid for much smaller $l_c/R_p$ than the corresponding expression for the slab and that although the lowest decay rates are of comparable magnitude the spacing between the decay rates is smaller by a factor of $\sqrt{l_c/R_p}$. This means that the time at which simple $e^{-t}$ behavior occurs is correspondingly longer.

The same method can be used to find the lowest eigenstates of the Torrey equation in a sphere for small $l_c/R_p$. They turn out to be caps at the North and South poles with Airy functions in the radial direction but this time the polar angular function satisfies the confluent hypergeometric equation. The lowest-order approximation to the magnetization of the left wall states is

$$m_0=\mathrm{Ai}[e^{+2\pi i/3}(E_0-ih')]$$
$$\times(\theta'^2/2)^{|m|/2}e^{\theta'^2(1+i)/4+im\phi}L_n^{|m|}[(1+i)\theta'^2/2]. \tag{24}$$

Here $R_p$ is the radius of the sphere, $h'$ and $\theta'$ are defined in exactly the same way as for the cylinder except that $r$ is the radial coordinate of the sphere, and $\theta$ is the polar angle. $\phi$ is the azimuthal angle, $m$ is an integer, and $n$ is a positive integer. $L_n^{|m|}$ is the generalized Laguerre polynomial (as defined in Ref. 19). The corresponding eigenvalues are

$$E_{i,n,m}=-igR_p+g^{2/3}D_0^{1/3}e^{-2\pi i/3}a_i+\sqrt{gD_0/R_p}(1+i)$$
$$\times(2n+1+|m|)+\mathcal{O}(g^{1/3}D_0^{2/3}/R_p). \tag{25}$$

Unlike the $l_c\gg R_p$ regime where the long-lived states are sensitive to the whole pore the above ideas should in fact hold for more general geometries since the magnetization at long times will be confined to pools where there is a dimple in the wall perpendicular to the gradient direction. $R_p$ will be

replaced by the radii of curvature of the dimple. The result for the cylinder is thus the correct asymptotic form for the decay rates and eigenstates in the dimples in a general two-dimensional pore space. The most general dimple in three dimensions has different principal radii of curvature. We thus expect the degeneracy for the sphere of the angular contributions to the decay rates to be lifted. In the language of quantum mechanics it is clear that, in going from the cylinder to the sphere, the extra angular degree of freedom has resulted, to lowest order, in producing the eigenstates of a two-dimensional harmonic oscillator. Thus a general dimple in three dimensions with principal radii of curvature $R_1$ and $R_2$ will have, to lowest order, decay rates corresponding to two oscillators of different frequency:

$$E_{i,j,k}=+iR_pg+g^{2/3}D_0^{1/3}e^{-2\pi i/3}a_i+\sqrt{gD_0/R_1}(j+1/2)\times(1+i)+\sqrt{gD_0/R_2}(k+1/2)(1+i)+\cdots . \quad (26)$$

Here $R_p$ is the Cartesian distance from the extremum of the dimple to the center of the pore space in the direction of the gradient. Clearly the radial levels and thus the gross magnitude of the lowest decay rate are unaltered for a general dimple in two or three dimensions. We therefore find independent of pore shape the universal long-time decay rate $\ln|M(z,t)|\sim -E_1g^{2/3}D_0^{1/3}t$, where $E_1$ is a constant $\sim 0.5094$ in the limit $R_p\gg l_c$. It is important to ask whether for some general pore if we are ever in the regime where the above results are valid. The real criterion is not that $R_{1,2}\gg l_c$ for every dimple in the wall but merely for some, i.e., that there is a separation of length scales. Roughness or dimples on length scales much less than $l_c$ will be in the fast diffusion limit and should not grossly affect the results.

## IV. IMPLICATIONS FOR THE HAHN SPIN-ECHO EXPERIMENT

The above results are concerned with theoretical considerations of the free induction decay following a $\pi/2$ pulse. In this section we focus on the implications for experimental measurements. The experimental quantity of interest is the Hahn spin echo, since for short times the free induction signal is not killed by the real "decay" parts of the eigenvalues but by the rapid dephasing between states caused by their imaginary oscillatory parts. This phenomenon, known as inhomogeneous broadening, is nearly eliminated with the Hahn echo. To calculate the echo amplitude we take the complex conjugate of the magnetization at a time $t=\tau$ corresponding to the application of a $\pi$ pulse. To see how it evolves from there to the echo at $t=2\tau$ we must use the Greens function:[8]

$$G(\mathbf{r},\mathbf{r}',t)=\sum N_im_i(\mathbf{r})m_i(\mathbf{r}')e^{-E_it}, \quad (27)$$

where $N_i$ is a normalization factor. The resulting magnetization must be integrated over to obtain the echo amplitude. If we start with uniform magnetization at $t=0$, then the echo amplitude is

$$\mathcal{M}(2\tau)=\sum_{i,j} N_i^*N_jc_i^*c_jO_{ij}\exp[-(\Gamma_i+\Gamma_j)\tau-i(\omega_j-\omega_i)\tau)], \quad (28)$$

where $c_i=\int m_i(\mathbf{r})d\mathbf{r}$ and the overlap $O_{ij}=\int m_i^*(\mathbf{r})m_j(\mathbf{r})d\mathbf{r}$. $\Gamma_i$ and $\omega_i$ are are the real and imaginary parts of $E_i$. In most of the magnetic resonance systems which have been studied the eigenstates $m_i$ are real (as is the case in the $l_c\gg R_p$ limit) so that orthogonality then ensures that the matrix $O_{ij}$ is diagonal and there are no oscillatory terms in the echo amplitude. This is certainly not the case when $l_c<R_p$ but it should be noted that such oscillations are of low frequency and do not contribute strongly to the decay of the echo amplitude. This can be seen from the fact that the elements $O_{ij}$ are small unless states $i$ and $j$ are physically localized in the same region of space so that $\omega_i\sim\omega_j$ if we assume $\omega_i$ to be a kind of average Larmor frequency for the eigenstate. Clearly at long enough times the echo amplitude becomes a pure exponential decay.

We now consider the prospects of experimentally quantitatively observing the decay rates calculated above. We argue that these are good in the case $l_c\gg R_p$ but slim for the case $l_c\ll R_p$ outside of the one-dimensional slab geometry.

First the case $l_c\gg R_p$. The crossover time at which pure decay sets in is of the order $R_p^2/D_0$. Note this is also the time scale at which the unbounded space formula breaks down. Inserting the decay rate $R_p^4g^2/D_0$, we find the signal strength at crossover is of order $\exp[-\mathcal{O}R_p^6g^2/D_0^2]$. The exponent is a small parameter and so not much signal will be lost by crossover. In addition to this the preexponential factors will be near unity because the lowest eigenstate is similar to the diffusive ground state (a constant in space) which is what the system starts in at $t=0$. So in conclusion as $R_p/l_c\to 0$ the proportion of signal lasting to the pure decay regime tends to unity (neglecting bulk $T_2$, etc.).

Now consider the regime $l_c\ll R_p$. In this case the crossover time depends on the dimensionality: $\tau\sim g^{-2/3}D_0^{-1/3}$ for the one-dimensional slab, $\tau\sim\sqrt{R_p/gD_0}$ in two dimensions or above. Note that in one dimension this is also the time scale at which the unbounded space formula breaks down but in higher dimension there is an intermediate regime $g^{-2/3}D_0^{-1/3}<\tau<\sqrt{R_p/gD_0}$ in which decay is neither pure cubic or pure linear. Inserting the decay rates we find the signal remaining at crossover is $\exp[-\mathcal{O}(1)]$ for the slab and $\exp[-\sqrt{R_p/l_c}]$ for the cylinder. However, in this regime the prefactors in front of the exponentials may be the dominant effect. For the diagonal terms these, loosely speaking, represent the volume fraction of the pore space that is occupied by the eigenstate. For $l_c\ll R_p$ the longest lived states are squashed into the dimples in the pore walls and represent only a tiny volume fraction thus yielding a negligible signal. (Although clearly the one-dimensional geometry is a special case—we expect to be in the $l_c\ll R_p$ regime even if $l_c/R_p$ is as big as 1/5 in which case the longest lived states are quite large.) So as $l_c/R_p\to 0$ the proportion of signal remaining at the pure decay regime goes to zero. We expect in general for small but finite $l_c/R_p$ that $\ln[\mathcal{M}(2\tau)/\mathcal{M}(0)]$ will bottom out from the $-\tau^3$ falloff but never measurably become linear

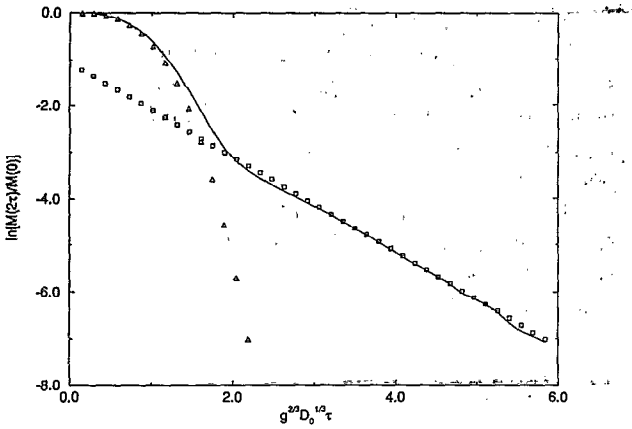


FIG. 2. Numerical simulation of the Hahn spin-echo envelope in the one-dimensional slab geometry. $R_p/l_c=17.1$. Also plotted are the short-time formula $-2D_0g^2\tau^3/3$, and the long-time decay rate $-0.5094D^{1/3}g^{2/3}2\tau$. The intercept for the latter was obtained by fit to the data.

with time. The angular decay levels never quite resolve themselves and we get stuck in the intermediate regime.

We have investigated the $l_c<R_p$ regime with random walk simulations. Some results are shown in Figs. 2 and 3. As expected the results in one dimension are in clear agreement with the short- and long-time behavior predicted above. For the cylindrical geometry we could not simulate low enough signal levels to capture the pure exponential regime.

The intermediate regime between the two limits is of course where many experiments will be performed. In this case we cannot say anything quantitative about the long-time behavior. However, there is potential structural information obtainable from the qualitative observation that if the pore is larger than $l_c$ in the direction of the gradient it is clearly $l_c$ that will confine the packet of magnetization at long times in that direction and not the pore wall separation. This is consistent with the conclusion from Sec. II that the commonly used $e^{-(2/3)D_0g^2\tau^3}$ result is only valid until spins diffuse over a length $l_c$ or $R_p$, whichever is smaller.

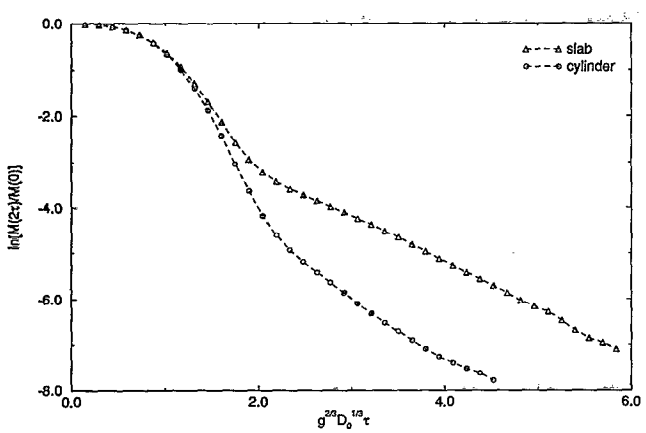


FIG. 3. Numerical simulation of the Hahn spin echo for the one-dimensional slab geometry as compared to the cylindrical one. $R_p/l_c=17.1$ in both cases if we take $R_p$ to be the **diameter** of the cylinder.

## V. IMPLICATIONS FOR THE EDGE ENHANCEMENT OF IMAGES

We now discuss the implications for diffusive edge enhancement of images. By this we mean the brightening of frequency encoded images around obstructions to diffusion. We discuss this from the point of view of eigenstates of the Torrey equation which helps to clarify the theoretical picture.

We assume for simplicity that in any one pulse sequence there is a read frequency encoding gradient effectively permanently on in one direction and that imaging in the other directions is by negligibly short slice selective gradient pulses, or will be effected by projection reconstruction. It is possible to use phase encoding in the other directions if the phase encoding gradient pulse is short enough, as in the experiments of Callaghan. However, this seriously complicates theoretical understanding. The other techniques mentioned above are simpler because the results of any one pulse sequence are only concerned with imaging in one dimension at a time.

To obtain the one-dimensional image in the read direction one can either Fourier transform the time envelope of the free induction decay as in the numerical study of Putz *et al.*[15] or the envelope of the Hahn echo as in the work of Callaghan.[2] Consider first imaging via Fourier transformation of the free induction decay in the presence of a one-dimensional read gradient. If there is no diffusion and neglecting bulk decay effects the magnetization density just rotates at the local Larmor frequency. $M(\mathbf{r},t)=M(\mathbf{r},0)\times\exp(-i\mathbf{g}\cdot\mathbf{r}t)$. The integral of this over space is the observed signal $S(t)$. So calculating $2\,\mathrm{Re}[\int_0^\infty S(t)\times\exp(+igtx)dg\ t]$ yields the function $M(\mathbf{r},0)$ integrated over the directions perpendicular to the gradient. When there is diffusion the signal is

$$S(t)=\sum c_iN_ie^{-(\Gamma_i+i\omega_i)t}. \tag{29}$$

Evaluating the above integral we obtain for the image

$$M(x,0)=\sum \frac{2c_iN_i\Gamma_ig}{(gx-\omega_i)^2+\Gamma_i^2}. \tag{30}$$

Consider the one-dimensional geometry. The image for a large value of $R_p/l_c$ is a sum of many Lorentzians. From the above results and the work of Stoller *et al.* it is clear that the sum consists of peaks becoming successively sharper as the peaks become closer to the wall. There is an infinite number of broad low amplitude peaks at the center of the box which will obscure some of this structure. This description is the theoretical basis for Fig. 3(a) in Ref. 15 and Fig. 1 of Ref. 14. The quality of these simulations is such that only the peaks nearest to the walls were resolved. These peaks correspond to the terms in Eq. (30) that come from the lowest decay rates given by Eq. (17). It is of interest to note that the shape of the peak in Fig. 3(d) of Ref. 15 which is approaching the regime $R_p\ll l_c$ is well approximated by a single term in Eq. (30). The corresponding $\Gamma_1$ can be read off from the results of Neumann[4] to be $\Gamma_1=g^2R_p^4/(120D_0)$. The transition between these two regimes requires a full discussion of the work of Stoller *et al.*.

Now consider imaging via the Hahn echo. We define $\delta=t-2\tau$ where $2\tau$ is the echo time. Now if there is no diffusion the Hahn echo and free induction signals are the same, i.e., $S(t)=\mathcal{M}(\delta)$. However, if there is diffusion and if for simplicity we neglect the off-diagonal terms in the matrix $O_{ij}$ we find from Eq. (28):

$$\mathcal{M}(\delta)=\sum |c_i|^2|N_i|^2O_{ii}e^{-2\Gamma_i\tau-\Gamma_i\delta-i\omega_i\delta}. \tag{31}$$

If we now calculate $2\,\mathrm{Re}[\int_0^\infty \mathcal{M}(\delta)\exp(+ig\,\delta x)dg\ \delta]$ we obtain for the image

$$M(x,0)=\sum \frac{2g|c_i|^2|N_i|^2O_{ii}e^{-2\Gamma_i\tau}\Gamma_i}{(gx-\omega_i)^2+\Gamma_i^2}. \tag{32}$$

We see from this result that due to the decay term $e^{-2\Gamma_i\tau}$ the eigenstates with spectral weight further from the walls (and thus larger $\Gamma_i$) contribute less and less at increasing $\tau$. Thus in the limit of long echo times the image becomes two Lorentzians localized near to the walls which are derived from the decay rates of Eq. (17). It should be emphasized that Eq. (32) is clearly not an image of the magnetization. While the magnetization is given by Airy functions and is maximum at the wall, the Lorentzian peaks in the image are displaced in from the sides of the container because of the imaginary part of $\exp(-2\pi i/3)a_i$ in Eq. (17). This extra edge enhancement in the Hahn echo is what was observed in the experiments of Callaghan. In Ref. 2 the extra enhancement of the Hahn echo was taken to occur by a different mechanism than the simulations based on the FID.

## VI. CONCLUSIONS

In this paper we have identified two routes by which the Hahn echo formula (1) for unbounded space breaks down. There is a well defined temporal regime in a bounded space where this formula remains valid.

We have extensively drawn on the work of Stoller *et al.*,[8] which gives rigorous results for the one-dimensional slab geometry. We have generalized their results to higher dimension and find in the asymptotic limit $R_p \gg l_c$ a universal long-time decay rate. We propose that $l_c$ limits the effective pore size.

Based on the above results we were able to provide a simple interpretation of the diffusive edge enhancement of NMR images which has been observed both in simulation and experiment.

## ACKNOWLEDGMENTS

We are grateful to B. I. Halperin, P. P. Mitra, L. Schwartz, H. Stone, and particularly M. Hurlimann for numerous useful discussions.

[1] J. A. Glasel and K. H. Lee, J. Am. Chem. Soc. **96**, 970 (1974).
[2] P. T. Callaghan, A. Coy, L. Ford, and C. Rofe, J. Magn. Reson. A **101**, 347 (1993).
[3] L. L. Latour, P. P. Mitra, R. L. Kleinberg, and C. H. Sotak, J. Magn. Reson. A **101**, 342 (1993).
[4] C. H. Neumann, J. Chem. Phys **60**, 4508 (1974).
[5] J. S. Murday and R. M. Cotts, J. Chem. Phys. **48**, 4938 (1968).
[6] J. C. Tarczon and W. P. Halperin, Phys. Rev. B **32**, 2798 (1985).
[7] P. Le Doussal and P. N. Sen, Phys. Rev. B **46**, 3465 (1992).
[8] S. D. Stoller, W. Happer, and F. J. Dyson, Phys. Rev. A **44**, 7459 (1991).
[9] E. L. Hahn, Phys. Rev. **80**, 580 (1950).
[10] P. Bendel, J. Magn. Reson. **86**, 509 (1990).
[11] R. C. Wayne and R. M. Cotts, Phys. Rev. **151**, 264 (1966).
[12] B. Robertson, Phys. Rev. **151**, 273 (1966).
[13] R. L. Kleinberg and M. A. Horsfield, J. Magn. Reson. **88**, 9 (1990).
[14] W. B. Hyslop and P. C. Lauterbur, J. Magn. Reson. **94**, 501 (1991).
[15] B. Putz, D. Barsky, and K. Schulten, J. Magn. Reson. **97**, 27 (1992).
[16] P. P. Mitra, P. N. Sen, and L. M. Schwartz, Phys. Rev. B **47**, 8565 (1993).
[17] T. M. de Swiet (unpublished).
[18] H. C. Torrey, Phys. Rev. **104**, 563 (1956).
[19] M. Abramowitz and I. A. Stegun, *Handbook of Mathematical Functions* (Dover, New York, 1965).